International Journal of Electrical and Computer Engineering (IJECE)
Vol. 16, No. 2, April 2026, pp. 587~597
ISSN: 2088-8708, DOI: 10.11591/ijece.v16i2.pp587-597

Identification of critical buses in the Sulbagsel electrical system network integrated with wind power plants

Andi Muhammad Ilyas[1], Agus Siswanto[2], Muhammad Natsir Rahman[1]
[1]Department of Electrical Engineering, Faculty of Engineering, Khairun University, Ternate, Indonesia
[2]Department of Electrical Engineering, Faculty of Engineering, 17 Agustus 1945 University, Cirebon, Indonesia

Article Info

Article history:

Received Apr 6, 2025
Revised Nov 27, 2025
Accepted Jan 15, 2026

Keywords:

Hybrid stability index
Identification of critical buses
Network stability
Sulbagsel 78-bus system
Wind power plants

ABSTRACT

The growing deployment of renewable energy has become increasingly important as conventional fossil-based generation faces sustainability and resource limitations. On Sulawesi Island, Indonesia, wind energy contributes to the regional grid through several wind power plants, whose fluctuating generation introduces operational concerns for system stability. This study investigates the stability performance of the Sulbagsel 78-bus network by pinpointing vulnerable buses and examining the effects of wind power variability. A hybrid stability index (HSI), which integrates multiple stability indicators, is applied to obtain a more robust assessment. The analysis shows that the entire system operates within a secure margin, with all index values remaining below the critical limit (<1). The most sensitive areas are located on the transmission paths connecting Bus 56 Sidera–Bus 57 Sidera 70 kV (0.02268), Bus 38 Bosowa–Bus 40 Pangkep (0.02220), and Bus 73 Powatu 150 kV–Bus 74 Powatu 70 kV (0.02187). In contrast, the Bus 24 Tanjung Bunga–Bus 25 Bontoala corridor demonstrates the strongest stability margin (0.00026). These results indicate that the variability of wind generation does not impose significant negative impacts on the overall stability of the Sulbagsel power system.

Corresponding Author:

Andi Muhammad Ilyas
Department of Electrical Engineering, Faculty of Engineering, Khairun University
Jln. Jusuf Abdulrahman, Kampus Gambesi, Ternate, Maluku Utara 97719, Indonesia
Email: aamilyas@gmail.com

1. INTRODUCTION

Voltage-related instability represents one of the most serious vulnerabilities in power networks, as it can trigger progressive voltage deterioration and ultimately lead to large-scale system failures. This concern is particularly relevant for the electrical grid on Sulawesi Island, Indonesia, where the increasing use of wind-based generation adds an additional layer of operational uncertainty. The output of wind turbines depends directly on naturally changing wind conditions, resulting in generation that is highly variable and less controllable than the steady supply typically offered by conventional fossil-fueled units. For this reason, rigorous mechanisms for observing system behavior and detecting early signs of instability are vital to maintain dependable operation of networks incorporating wind energy. As the global energy sector moves toward reducing reliance on fossil resources, a wide range of renewable technologies and storage solutions is being deployed. Within this transition, hybrid energy configurations have emerged as promising pathways for achieving cleaner power production while strengthening grid robustness and overall system adaptability [1]–[4].

Kundur [5] defines voltage stability as the capability of an electric power system to sustain acceptable voltage levels at all buses, both under steady-state conditions and in the aftermath of system disturbances. A well-designed power system is expected to preserve its equilibrium and respond adaptively

so that post-disturbance operating conditions remain within permissible limits [5]–[10]. Electricity has become a fundamental requirement of modern society, and the continuous growth in demand results in persistent changes in system operating patterns. At the same time, the penetration of renewable energy resources into traditionally fossil-based networks continues to increase. While this transition supports sustainability objectives, the integration of variable renewable generation introduces additional complexities in system operation and stability management [11]–[14].

Numerous analytical approaches have been proposed to evaluate voltage stability and to quantify the proximity of an operating point to instability through various voltage stability indices [15]–[17]. For practical application in planning and operational environments, such indices must be computationally efficient and straightforward to implement. These indicators enable system planners and operators to locate buses that exhibit weak voltage support in an interconnected network. In principle, voltage stability assessment in power systems serves four key purposes: i) detecting potential voltage depressions, ii) identifying the emergence of voltage instability, iii) determining vulnerable or weak buses within the network, and iv) pinpointing areas where instability is likely to develop.

This research utilizes operational data from the 78-bus Southern Sulawesi (Sulbagsel) power network to examine the system's voltage stability characteristics. The assessment is conducted using the hybrid stability index (HSI), an integrated indicator that combines the line stability index (Lmn) and the fast voltage stability index (FVSI) to provide a more refined and reliable evaluation of system conditions. The principal contribution of this work is the identification of vulnerable or stability-critical buses within the Sulbagsel network, along with an examination of how the variability of wind power generation influences overall system behavior when wind power plants are incorporated into the existing grid infrastructure. The results offer a detailed perspective on network susceptibility and elucidate the extent to which renewable generation intermittency affects power system performance.

The IEEE 30-bus test system, as documented in Hadi Saadat's "Power system analysis" [6], was employed as a benchmark dataset to validate the proposed approach. Simulations carried out on this test system were used to assess the precision and robustness of the HSI in detecting buses with critical stability margins. To extend the evaluation to a practical network, additional analyses were performed on the Sulbagsel 78-bus system, which incorporates a wind power plant within its operational configuration. This real-system case study allowed for a detailed examination of voltage stability. Figure 1 shows the single-line diagram of the IEEE 30-bus test system.

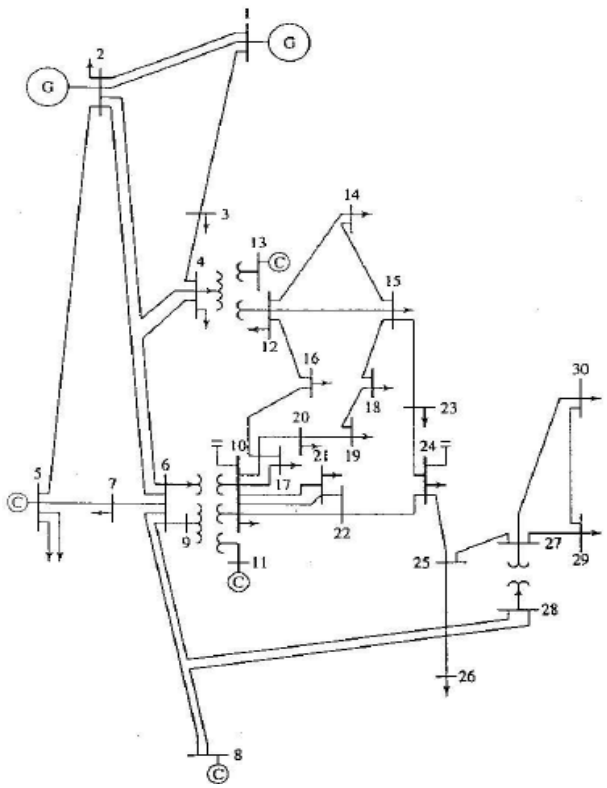

Figure 1. Single-line diagram of the IEEE 30-bus test system

The IEEE 30-bus system originates from the transmission network model developed by the American Electric Power Service Corporation, which has since become one of the most widely used benchmark systems in power system research. This dataset is routinely employed in the electrical engineering community as a standardized reference for evaluating analytical methods, validating simulation tools, and comparing the performance of various computational algorithms used to solve complex power system problems [6]. The model is composed of six generator buses, twenty-four load buses, and forty-one transmission lines or branches that interconnect the buses, forming a representative medium-scale network suitable for both academic studies and practical testing environments. Among the generator buses, Bus 1 functions as the slack or reference bus, providing the necessary balance between real and reactive power within the system. The configuration of the IEEE 30-bus system is traditionally illustrated through a one-line diagram, which presents the arrangement of generators, loads, transformers, and transmission lines in a simplified schematic form to facilitate power flow and stability analysis. The dataset utilized in this study corresponds to the Sulbagsel 78-bus power system as recorded in December 2023. Table 1 summarizes the key characteristics and operational parameters of the network.

Table 1. Summary of Sulbagsel 78-bus system data

Bus number	Bus code	Bus name	Bus number	Bus code	Bus name
1	1	Sengkang	40	0	Pangkep
2	0	Sidrap	41	0	Pangkep 70 kV
3	0	Soppeng	42	0	Barru
4	0	Enrekang	43	2	GI Balusu
5	2	Makale	44	0	Pare-pare
6	2	Palopo	45	2	PLTD Suppa
7	0	Siwa	46	2	Pinrang
8	2	PLTB Sidrap	47	0	Polmas
9	0	Bone	48	0	Majene
10	2	Sinjai	49	2	Bakaru
11	0	Bulukumba	50	0	Mamuju
12	0	Bantaeng Switch	51	0	Mamuju Baru
13	0	Bantaeng Smelter	52	2	PLTU Mamuju
14	0	Bantaeng New	53	0	Topoyo
15	0	Jeneponto	54	0	Pasang Kayu
16	2	PLTB Tolo	55	0	Silae
17	2	PLTU Jeneponto EXP	56	0	Sidera
18	2	PLTU Jeneponto	57	0	Sidera 70 kV
19	2	Punagaya	58	0	Poso
20	0	Tallasa	59	0	Pamona 150 kV
21	0	Sungguminasa	60	2	Tallise
22	0	Bolangi	61	0	Parigi
23	0	Maros	62	2	Pamona 275 kV
24	0	Tanjung Bunga	63	2	Slwna
25	0	Bontoala	64	0	Latupa 275 kV
26	0	Tallo Lama	65	0	Latupa 150 kV
27	0	Tallo Lama 70 kV	66	0	Wotu 275 kV
28	0	Bontoala 70 kV	67	0	Wotu 150 kV
29	2	Tello	68	0	Malili
30	0	Panakukang	69	0	Lasusua
31	0	Tello 30 kV	70	0	Kolaka
32	0	Barawaja	71	0	UNNHA
33	0	Tello 70 kV	72	0	Kendari
34	2	Borongloe	73	0	Pwatu 150 kV
35	0	Daya	74	0	Pwatu 70 kV
36	0	Mandai	75	2	NTNSA
37	0	Tonasa	76	2	PLTU Maramo
38	0	Kima	77	0	Andolo
39	0	Bosowa	78	0	Kasipute

Table 1 provides an overview of the Sulawesi Island power network, which comprises 78 buses, including 21 generator buses and 57 load buses. This arrangement represents the overall layout of the regional grid, incorporating multiple generation points and load centers distributed across the system. The Sulbagsel 78-bus network also contains 92 transmission lines that interconnect the buses. Additional information regarding the configuration of this network is presented in Table 2.

Table 2. Line data of the Sulbagsel 78-bus system

From bus		To bus		From bus		To bus	
1	Sengkang	2	Sidrap	35	Daya	36	Mandai
1	Sengkang	3	Soppeng	36	Mandai	41	Pangkep 70 kV
1	Sengkang	7	Siwa	37	Tonasa	41	Pangkep 70 kV
2	Sidrap	3	Soppeng	38	Kima	40	Pangkep
2	Sidrap	4	Enrekang	39	Bosowa	40	Pangkep
2	Sidrap	5	Makale	40	Pangkep	41	Pangkep 70 kV
2	Sidrap	8	PLTB Sidrap	40	Pangkep	42	Barru
2	Sidrap	44	Pare-pare	40	Pangkep	43	GI Balusu
3	Soppeng	9	Bone	42	Barru	43	GI Balusu
4	Enrekang	5	Makale	43	GI Balusu	44	Pare-pare
5	Makale	6	Palopo	44	Pare-pare	45	PLTD Suppa
6	Palopo	65	Latupa 275 kV	44	Pare-pare	46	Pinrang
8	PLTB Sidrap	23	Maros	44	Pare-pare	47	Polmas
9	Bone	10	Sinjai	46	Pinrang	49	Bakaru
9	Bone	11	Bulukumba	47	Polmas	48	Majene
10	Sinjai	11	Bulukumba	47	Polmas	49	Bakaru
11	Bulukumba	12	Bantaeng Switch	48	Majene	50	Mamuju
11	Bulukumba	15	Jeneponto	50	Mamuju	51	Mamuju Baru
12	Bantaeng Switch	13	Bantaeng Smelter	51	Mamuju Baru	52	PLTU Mamuju
14	Bantaeng New	15	Jeneponto	51	Mamuju Baru	53	Topoyo
15	Jeneponto	16	PLTB Tolo	53	Topoyo	54	Pasang Kayu
15	Jeneponto	19	Punagaya	54	Pasang Kayu	55	Silae
17	PLTU Jeneponto EXP	19	Punagaya	55	Silae	56	Sidera
18	PLTU Jeneponto	19	Punagaya	56	Sidera	57	Sidera 70 kV
19	Punagaya	20	Tallasa	56	Sidera	58	Poso
19	Punagaya	24	Tanjung Bunga	57	Sidera 70 kV	60	Tallise
20	Tallasa	21	Sungguminasa	58	Poso	59	Pamona 150 kV
21	Sungguminasa	22	Bolangi	59	Pamona 150 kV	62	Pamona 275 kV
21	Sungguminasa	23	Maros	60	Tallise	61	Parigi
21	Sungguminasa	24	Tanjung Bunga	62	Pamona 275 kV	63	Slwna
21	Sungguminasa	29	Tello	62	Pamona 275 kV	64	Latupa 275 kV
22	Bolangi	23	Maros	62	Pamona 275 kV	66	Wotu 275 kV
24	Tanjung Bunga	25	Bontoala	64	Latupa 275 kV	65	Latupa 150 kV
25	Bontoala	26	Tallo Lama	64	Latupa 275 kV	66	Wotu 275 kV
26	Tallo Lama	27	Tallo Lama 70 kV	66	Wotu 275 kV	67	Wotu 150 kV
26	Tallo Lama	29	Tello	67	Wotu 150 kV	68	Malili
27	Tallo Lama 70 kV	28	Bontoala 70 kV	68	Malili	69	Lasusua
29	Tello	30	Panakukang	69	Lasusua	70	Kolaka
29	Tello	31	Tello 30 kV	70	Kolaka	71	Unaha
29	Tello	33	Tello 70 kV	71	Unaha	72	Kendari
29	Tello	38	Kima	72	Kendari	73	Pwatu 150 kV
29	Tello	39	Bosowa	72	Kendari	76	PLTU Maramo
31	Tello 30 kV	32	Barawaja	73	Pwatu 150 kV	74	Pwatu 70 kV
33	Tello 70 kV	34	Borongloe	74	Pwatu 70 kV	75	NTNSA
33	Tello 70 kV	35	Daya	72	Kendari	77	Andolo
33	Tello 70 kV	36	Mandai	77	Andolo	78	Kasipute

2. METHOD

The HSI is a composite analytical approach that integrates the Lmn with the FVSI. In this research, the HSI is employed to detect stability-critical buses and to evaluate the influence of output intermittency from wind power plants on the voltage stability of the electrical network. To examine the effectiveness of the proposed method, a series of simulations is conducted on the IEEE 30-bus test system following the steps outlined below:

Stage 1: The IEEE 30-bus system is solved using the Newton–Raphson power flow method to establish the baseline operating conditions.

Stage 2: The Lmn index is computed in conjunction with the Newton–Raphson results to identify buses exhibiting low stability margins.

Stage 3: The FVSI index is applied, also supported by the Newton–Raphson solution, to determine critical buses for comparative evaluation.

Stage 4: The HSI, formed by combining Lmn and FVSI within the Newton–Raphson framework, is utilized to validate the performance of the hybrid approach and to refine the identification of weak buses.

Stage 5: The verified HSI method is then implemented on the Sulbagsel 78-bus system as a real-network case study, enabling assessment of its scalability and accuracy in a larger, more complex grid environment.

2.1. Line stability index

The line stability index (Lmn) is formulated from the analytical characteristics of transmission-line power flow using a simplified single-line equivalent model. The index serves as an indicator of the voltage-stability margin for a transmission line that electrically links two buses in a power network [18]–[21]. In its formulation, the multi bus system is reduced into a single transmission line representation to enable easier derivation of the stability relationship between sending-end and receiving-end electrical quantities. This simplified model conceptually illustrated in Figure 2 is used to evaluate how close a line operates to its voltage collapse point.

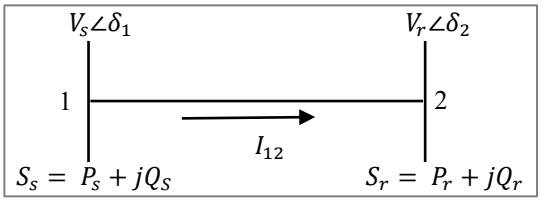

Figure 2. Single-line equivalent illustrating a transmission path

In this model, V_s, P_s, and Q_s refer to the voltage, active power, and reactive power at the sending side of the line, typically associated with the generator bus. Similarly, V_r, P_r, and Q_r correspond to the voltage, active power, and reactive power measured at the receiving side, which represents the load bus. The phase angle at the generator is denoted by δ_1, while δ_2 indicates the phase angle at the load side. The term I_{12} represents the current flowing from the sending end to the receiving end, and θ is the impedance angle of the transmission line. The mathematical formulation governing these quantities is presented as (1).

$$Lmn = \frac{4\ X\ Q_r}{|V_s|^2\ sin^2\ (\theta - \delta)} \leq 1 \quad (1)$$

The Lmn is directly influenced by reactive power and indirectly by active power through the voltage phase angle in the power system. This index is employed to assess the stability condition of a transmission line within the network. A line is considered to approach an unstable state when the Lmn value nears 1, indicating a potential disturbance or imbalance in power flow. Conversely, when the Lmn value remains below 1, the system is regarded as stable, signifying that the power flow is still within permissible limits for secure power system operation [20].

2.2. Fast voltage stability index

The fast voltage stability index (FVSI) is derived from the relationship between bus voltages and reactive power in the system. In its formulation, the sending-end bus is set as the reference with a zero-phase angle to simplify the analysis. FVSI is used to evaluate the voltage stability margin of a transmission line and is obtained from the general current expression between the sending bus ‘s’ and the receiving bus ‘r’ [22]–[25]. This index helps determine the potential for voltage instability under different loading and operating conditions. The formulation of the FVSI is presented as (2).

$$FVSI = \frac{4Z^2 Q_r}{V_s^2 X} \leq 1 \quad (2)$$

Where Z denotes the line impedance, X represents the line reactance, Q_r corresponds to the reactive power at the receiving bus, and V_s denotes the sending-end voltage magnitude. A transmission line is classified as critical when its FVSI value approaches unity, as this condition signifies a high susceptibility to voltage instability and the potential initiation of a system-wide collapse. The computation of FVSI therefore plays an important role in pinpointing the weakest bus within the network and in quantifying the remaining voltage stability margin under varying operating conditions.

2.3. Hybrid stability index

The hybrid stability index (HSI) is developed by integrating the Lmn [25], and the FVSI [26], to improve the precision and robustness of voltage stability assessment in power networks. By combining the fundamental parameters embedded within both indices, the HSI offers a broader and more reliable representation of system operating margins under varying load and generation conditions. All variables used in the formulation of the HSI are expressed in per-unit (p.u.) to ensure computational consistency and facilitate

comparative analysis across different components of the electrical system [27]–[29]. The simplified single-line configuration used in deriving and applying the HSI is illustrated in Figure 3.

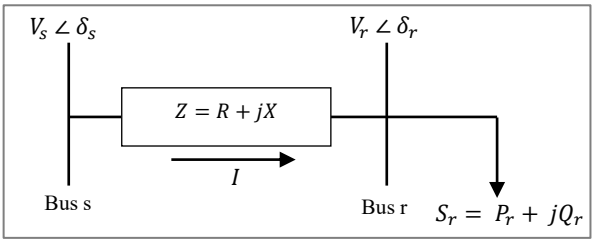

Figure 3. Two-bus system configuration shown in a single-line format

The mathematical formulation of the HSI is derived by combining the Lmn with the FVSI, enabling a more precise evaluation of voltage stability within the power network. This composite index integrates key operational variables to detect emerging instability conditions across the system. The complete mathematical representation of the HSI is provided below.

$$HSI = \frac{4Q_r}{|V_s|^2}\left[\frac{(|Z|)^2}{X}\sigma - \frac{X}{sin^2(\theta-\delta}(\sigma - 1)\right] \leq 1 \quad (3)$$

$$\sigma = \begin{cases} 1 & \delta < \delta c \\ 0 & \delta \geq \delta c \end{cases}$$

Note: σ functions as a modifier factor. Where σ represents a transition parameter whose value varies according to the magnitude of the phase-angle difference δ.

The research workflow outlining the sequential stages and methodological procedures employed in this study is shown in Figure 4. This diagram provides a structured overview of the research activities, starting from data acquisition, continuing through the analytical processes using the selected stability indices, and concluding with the interpretation of the resulting findings.

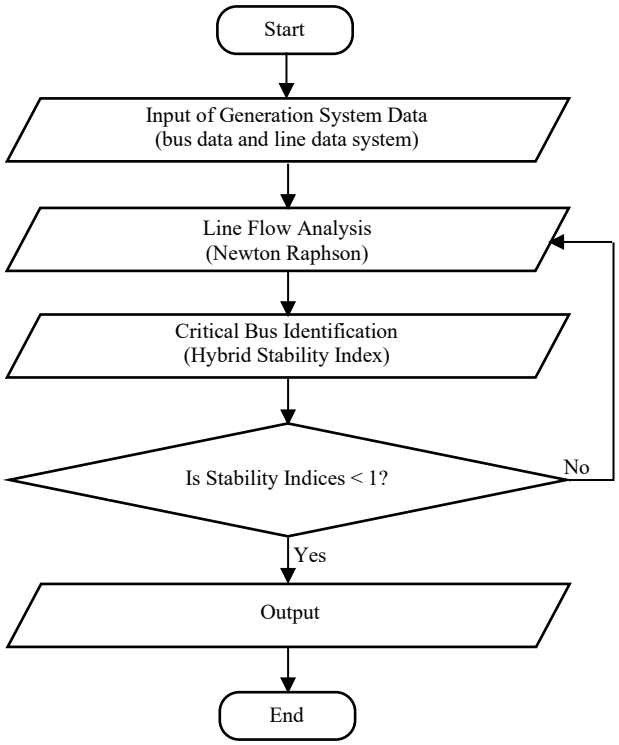

Figure 4. Research methodology flowchart

3. RESULTS AND DISCUSSION

The identification of critical buses and the evaluation of power-generation intermittency from wind power plants in this study were carried out through a two-stage analysis. In the first stage, the IEEE 30-bus benchmark system was employed to verify the robustness and accuracy of the stability assessment methods applied. In the second stage, the 78-bus Southern Sulawesi (Sulbagsel) power network integrated with the Sidrap and Jeneponto wind power plants was examined as a practical case study. This phase focuses on determining the system's weak buses and assessing the influence of wind power variability on overall system stability and operational performance.

3.1. IEEE 30-bus system stability

The stability analysis of the IEEE 30-bus test system was conducted to verify the reliability, consistency, and computational accuracy of the HSI in detecting critical buses within the network. This evaluation functions as a fundamental validation stage to confirm that the proposed index can reliably represent system stability across different loading scenarios and operational variations. In addition, Table 3 and the graphical outputs in Figure 5 provide a detailed quantitative characterization of the voltage stability profile of the IEEE 30-bus system based on HSI results. These findings offer a comprehensive representation of system behavior and support a more rigorous assessment of the relative criticality of each bus in the network.

Table 3. HSI results for the IEEE 30-bus system

Line number	From Bus	To Bus	HSI	Line number	From Bus	To Bus	HIS
1	1	2	0.00015	22	15	18	0.00064
2	1	3	0.00048	23	18	19	0.00038
3	2	4	0.00047	24	19	20	0.00020
4	3	4	0.00010	25	10	20	0.00058
5	2	5	0.00054	26	10	17	0.00022
6	2	6	0.00049	27	10	21	0.00021
7	4	6	0.00011	28	10	22	0.00043
8	5	7	0.00033	29	21	22	0.00007
9	6	7	0.00022	30	15	23	0.00059
10	6	8	0.00011	31	22	24	0.00060
11	6	9	0.00051	32	23	24	0.00080
12	6	10	0.00138	33	24	25	0.00106
13	9	11	0.00048	34	25	26	0.00134
14	9	10	0.00025	35	25	27	0.00065
15	4	12	0.00064	36	28	27	0.00098
16	12	13	0.00032	37	27	29	0.00128
17	12	14	0.00071	38	27	30	0.00185
18	12	15	0.00037	39	29	30	0.00145
19	12	16	0.00055	40	8	28	0.00054
20	14	15	0.00103	41	6	28	0.00016
21	16	17	0.00053		Average		0.00058

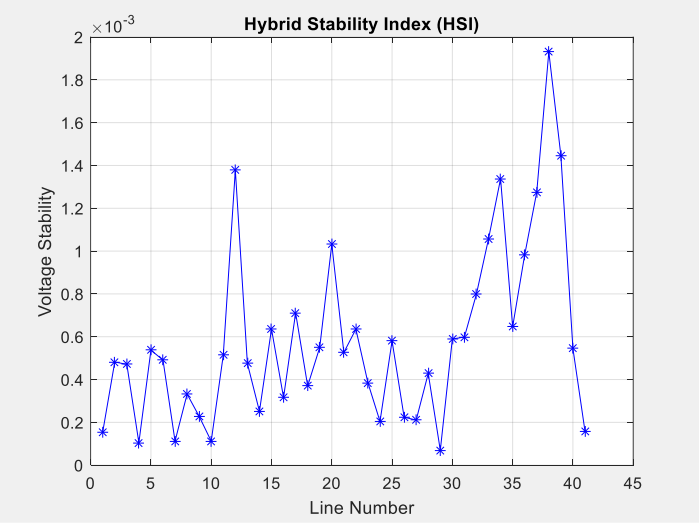

Figure 5. Graph of the IEEE-30 bus system stability index based on the HSI index method

Overall, the stability evaluation of the IEEE 30-bus network using the HSI confirms that the system operates within a secure and stable region. The lowest HSI value, approximately 0.00007, occurs on Line 29 connecting Bus 21 and Bus 22, indicating the strongest stability margin in the system. In contrast, the highest HSI value 0.00185 is recorded on the line linking Bus 29 to Bus 30, identifying this segment as the most vulnerable within the network. The computed average HSI value of 0.00058 further supports the conclusion that the system remains well below any critical threshold. To provide a clearer interpretation, the distribution of HSI values for all transmission lines is depicted in Figure 5.

3.2. Stability of the Sulbagsel 78-bus system

The stability evaluation of the Sulawesi 78-bus electric power network was conducted using the HSI to identify critical buses within the Southern Sulawesi (Sulbagsel) transmission system, which has been integrated with wind power plants [30], [31]. This assessment provides insight into the most vulnerable locations in the network and offers a more comprehensive characterization of the system's operational behavior under diverse loading and generation scenarios. In addition, the study examines the impact of wind power generation intermittency on overall system stability, recognizing the variability inherent to wind resources and its influence on voltage magnitudes, reactive power demand, and real power transfer capability. The results of the critical bus identification, together with the observed effects of wind power plants output fluctuations on system performance, are presented in Table 4.

Table 4. Critical bus identification in the Sulbagsel 78-bus transmission system using the HSI method

From bus	To bus	Without PLTB	PLTB 11:00 AM	PLTB 8:00 PM	From bus	To bus	Without PLTB	PLTB 11:00 AM	PLTB 8:00 PM
1	2	0.00318	0.00318	0.00318	35	36	0.00381	0.00381	0.00381
1	3	0.00239	0.00239	0.00239	36	41	0.01823	0.01823	0.01823
1	7	0.00476	0.00476	0.00476	37	41	0.00270	0.00270	0.00270
2	3	0.00409	0.00409	0.00409	38	40	0.00284	0.00284	0.00284
2	4	0.00366	0.00366	0.00366	39	40	0.00162	0.00162	0.00162
2	5	0.00742	0.00742	0.00742	40	41	0.01586	0.01586	0.01586
2	8	0.00064	0.00064	0.00064	40	42	0.00375	0.00375	0.00375
2	44	0.00145	0.00145	0.00145	40	43	0.00350	0.00350	0.00350
3	9	0.00322	0.00322	0.00322	42	43	0.00213	0.00213	0.00213
4	5	0.00373	0.00373	0.00373	43	44	0.00345	0.00345	0.00345
5	6	0.00246	0.00246	0.00246	44	45	0.00058	0.00058	0.00058
6	65	0.00568	0.00568	0.00568	44	46	0.00203	0.00203	0.00203
8	23	0.00584	0.00584	0.00584	44	47	0.00726	0.00726	0.00726
9	10	0.00590	0.00591	0.00590	46	49	0.00467	0.00467	0.00467
9	11	0.01084	0.01085	0.01084	47	48	0.00381	0.00381	0.00381
10	11	0.00500	0.00500	0.00500	47	49	0.00381	0.00381	0.00381
11	12	0.00059	0.00059	0.00059	48	50	0.01104	0.01105	0.01104
11	15	0.00360	0.00359	0.00360	50	51	0.00450	0.00450	0.00450
12	13	0.00197	0.00197	0.00197	51	52	0.00509	0.00509	0.00509
14	15	0.00186	0.00186	0.00186	51	53	0.00696	0.00696	0.00696
15	16	0.00257	0.00257	0.00257	53	54	0.00706	0.00706	0.00706
15	19	0.00238	0.00239	0.00238	54	55	0.00749	0.00749	0.00749
17	19	0.00218	0.00218	0.00218	55	56	0.00250	0.00250	0.00250
18	19	0.00215	0.00215	0.00215	56	57	0.02268	0.02268	0.02268
19	20	0.00131	0.00131	0.00131	56	58	0.00744	0.00744	0.00744
19	24	0.00109	0.00109	0.00109	57	60	0.00701	0.00701	0.00701
20	21	0.00118	0.00118	0.00118	58	59	0.00715	0.00715	0.00715
21	22	0.00052	0.00052	0.00052	59	62	0.00564	0.00564	0.00564
21	23	0.00245	0.00245	0.00245	60	61	0.00749	0.00749	0.00749
21	24	0.00087	0.00087	0.00087	62	63	0.00272	0.00272	0.00272
21	29	0.00056	0.00056	0.00056	62	64	0.00321	0.00321	0.00321
22	23	0.00192	0.00192	0.00192	62	66	0.00174	0.00174	0.00174
24	25	0.00026	0.00026	0.00026	64	65	0.00548	0.00548	0.00548
25	26	0.00193	0.00193	0.00193	64	66	0.00158	0.00158	0.00158
26	27	0.01680	0.01680	0.01680	66	67	0.00558	0.00558	0.00558
26	29	0.00045	0.00045	0.00045	67	68	0.00306	0.00306	0.00306
27	28	0.00306	0.00306	0.00306	68	69	0.00503	0.00503	0.00503
29	30	0.00029	0.00029	0.00029	69	70	0.00488	0.00488	0.00488
29	31	0.02220	0.02220	0.02220	70	71	0.00422	0.00422	0.00422
29	33	0.01681	0.01681	0.01681	71	72	0.00293	0.00293	0.00293
29	38	0.00062	0.00062	0.00062	72	73	0.00080	0.00080	0.00080
29	39	0.00261	0.00261	0.00261	72	76	0.00506	0.00506	0.00506
31	32	0.01339	0.01339	0.01339	73	74	0.02187	0.02187	0.02187
33	34	0.00928	0.00928	0.00928	74	75	0.00479	0.00479	0.00479
33	35	0.00280	0.00280	0.00280	72	77	0.01228	0.01228	0.01228
33	36	0.00576	0.00576	0.00576	77	78	0.01237	0.01237	0.01237

The results presented in Table 4 summarize the identification of critical buses and the evaluation of voltage stability performance in the 78-bus Southern Sulawesi (Sulbagsel) power system under wind power generation intermittency. The analysis reveals that the most critical condition in the network occurs on the transmission segment connecting Bus 56 Sidera to Bus 57 Sidera 70 kV, which records the highest HSI value of 0.02268. The second highest criticality is observed on the line between Bus 38 Bosowa and Bus 40 Pangkep, with an HSI value of 0.02220, followed by the line between Bus 73 Powatu 150 kV and Bus 74 Powatu 70 kV, which yields an index of 0.02187. Conversely, the line exhibiting the strongest stability margin is the segment linking Bus 24 Tanjung Bunga and Bus 25 Bontoala, which presents the lowest HSI value of 0.00026. Overall, the Sulbagsel 78-bus network operates within a secure stability range, as all computed HSI values remain significantly below the critical threshold (HSI < 1). These findings demonstrate that, despite the inherent variability of wind power generation, the interconnected system maintains adequate voltage support and is capable of sustaining reliable power flow conditions.

To evaluate the influence of wind power plant generation intermittency on the stability of the Sulbagsel 78-bus power system, three simulation scenarios were conducted: i) a baseline scenario without wind power plant integration, ii) a scenario incorporating wind power plant generation data during the daytime peak-load period at 11:00 AM, and iii) a scenario utilizing wind power plant generation data during the nighttime peak-load period at 08:00 PM. The critical-bus identification results presented in the preceding table indicate that variations in wind power plant output do not exert a significant impact on the stability of the Sulbagsel 78-bus system. This suggests that the system remains robust under the observed levels of wind power plant intermittency.

This study provides a detailed assessment of the stability profile of each bus within the integrated power system, ranging from those exhibiting high vulnerability to instability to those classified as stable or non-critical. The results reinforce the contribution of this research, particularly in the systematic identification of critical or weak buses in the Sulbagsel 78-bus network and in the evaluation of the effects of wind power plant intermittency on the performance of the existing conventional grid.

4. CONCLUSION

Conclusions drawn from the critical-bus assessment and the evaluation of wind-generation intermittency using the HSI are summarized as follows: i) Analysis of the 78-bus Sulbagsel transmission network confirms that the system operates within a secure stability region. All computed HSI values remain significantly below the critical limit (<1); ii) The multi scenario simulations comprising conditions without wind power plant integration, with daytime wind generation, and with nighttime wind generation demonstrate that fluctuations in wind power plant output do not introduce a material degradation in system stability; iii) The bus-by-bus evaluation validates that the Sulbagsel 78-bus configuration exhibits acceptable stability margins across the entire network.

FUNDING INFORMATION

This work was conducted without external financial assistance. No funding was provided by governmental agencies, industry partners, or non-profit organizations for the execution of the research or the preparation of the manuscript.

AUTHOR CONTRIBUTIONS STATEMENT

The study was conducted by three researchers, with the allocation of responsibilities and tasks summarized in the table below.

Name of Author	C	M	So	Va	Fo	I	R	D	O	E	Vi	Su	P	Fu
Andi Muhammad Ilyas	✓	✓	✓	✓	✓	✓	✓	✓	✓	✓	✓	✓	✓	✓
Agus Siswanto	✓			✓	✓			✓						
Muhammad Natsir Rahman	✓			✓	✓			✓						

C : **C**onceptualization
M : **M**ethodology
So : **So**ftware
Va : **Va**lidation
Fo : **Fo**rmal analysis
I : **I**nvestigation
R : **R**esources
D : **D**ata Curation
O : Writing - **O**riginal Draft
E : Writing - Review & **E**diting
Vi : **Vi**sualization
Su : **Su**pervision
P : **P**roject administration
Fu : **Fu**nding acquisition

CONFLICT OF INTEREST STATEMENT

The author declares that no conflicts of interest exist in relation to the design, execution, or reporting of this research work.

REFERENCES

[1] H. ur Rashid Khan, U. Awan, K. Zaman, A. A. Nassani, M. Haffar, and M. M. Q. Abro, "Assessing hybrid solar-wind potential for industrial decarbonization strategies: global shift to green development," *Energies*, vol. 14, no. 22, p. 7620, Nov. 2021, doi: 10.3390/en14227620.

[2] A. M. Ilyas, A. Suyuti, I. C. Gunadin, and S. M. Said, "Optimal power flow model integrated electric power system with wind power generation - case study: electricity system South Sulawesi-Indonesia," *International Journal of Intelligent Engineering and Systems*, vol. 15, no. 4, Aug. 2022, doi: 10.22266/ijies2022.0831.37.

[3] B. Ismail *et al.*, "New line voltage stability index (BVSI) for voltage stability assessment in power system: the comparative studies," *IEEE Access*, vol. 10, pp. 103906–103931, 2022, doi: 10.1109/ACCESS.2022.3204792.

[4] M. D. Jaramillo, D. F. Carrión, and J. P. Muñoz, "A novel methodology for strengthening stability in electrical power systems by considering fast voltage stability index under N − 1 scenarios," *Energies*, vol. 16, no. 8, p. 3396, Apr. 2023, doi: 10.3390/en16083396.

[5] P. S. Kundur, *Power system stability and control*, 2nd ed. McGraw Hill, 2022.

[6] H. Saadat, *Power system analysis*, 2nd ed. McGraw-Hill, 1999.

[7] S. Abe, Y. Fukunaga, A. Isono, and B. Kondo, "Power system voltage stability," *IEEE Power Engineering Review*, vol. PER-2, no. 10, pp. 39–40, Oct. 1982, doi: 10.1109/MPER.1982.5519897.

[8] A. Oukennou and A. Sandali, "Novel voltage stability index for electric power system monitoring," *International journal of electrical and computer engineering systems*, vol. 10, no. 1, pp. 1–9, Oct. 2019, doi: 10.32985/ijeces.10.1.1.

[9] V. Geekiyanage, "Power system stability improvement through grid forming inverters for high penetration of grid following inverter scenarios," Master's Program in Advanced Energy Solutions, Department of Electrical Engineering and Automation, Aalto University, 2023.

[10] T. Ilamparithi, "ECE 488: Electrical Power Systems — Faculty of Engineering Course Outline," Spring 2019, Faculty of Engineering, University of Victoria, Victoria, BC, Canada, 2019.

[11] X. Bai, L. Qu, and W. Qiao, "Robust AC optimal power flow for power networks with wind power generation," *IEEE Transactions on Power Systems*, vol. 31, no. 5, pp. 4163–4164, Sep. 2016, doi: 10.1109/TPWRS.2015.2493778.

[12] R. Ma, X. Li, W. Gao, P. Lu, and T. Wang, "Random-fuzzy chance-constrained programming optimal power flow of wind integrated power considering voltage stability," *IEEE Access*, vol. 8, pp. 217957–217966, 2020, doi: 10.1109/ACCESS.2020.3040382.

[13] Haripuddin, A. Suyuti, S. M. Said, and Y. S. Akil, "Hybrid optimization method for thermal-wind integration with multi objective dynamic economic dispatch," *International Journal of Advanced Science and Technology*, vol. 29, no. 3, pp. 14958–14974, 2020.

[14] X. Lu, H. Wang, J. Zhang, Z. Han, and S. Qi, "Load forecasting method for power distribution networks oriented towards time series simulation with deep learning method," *Applied Mathematics and Nonlinear Sciences*, vol. 9, no. 1, 2024.

[15] K. Doğanşahin, "A new line stability index for voltage stability analysis based on line loading," *Clean Energy Technologies Journal*, vol. 1, no. 1, pp. 23–30, 2023, doi: 10.14744/cetj.2023.0004.

[16] S. Mokred, Y. Wang, and T. Chen, "A novel collapse prediction index for voltage stability analysis and contingency ranking in power systems," *Protection and Control of Modern Power Systems*, vol. 8, no. 1, pp. 1–27, Jan. 2023, doi: 10.1186/s41601-023-00279-w.

[17] I. Robandi, M. A. Prakasa, M. R. Djalal, A. Ramadhani, V. L. B. Putri, and R. S. Wibowo, "Stability improvement of hybrid renewable energy systems by using virtual inertia controller based on optimized FOPID with Harris Hawk optimization," *International Journal of Intelligent Engineering and Systems*, vol. 17, no. 5, pp. 770–782, Oct. 2024, doi: 10.22266/ijies2024.1031.58.

[18] M. Moghavvemi and F. M. Omar, "A line outage study for prediction of static voltage collapse," *IEEE Power Engineering Review*, vol. 18, no. 7, pp. 52–54, Jul. 1998, doi: 10.1109/39.691721.

[19] I. Samuel, J. Katende, S. A. Daramola, and A. Awelewa, "Review of system collapse incidences on the 330-kV Nigerian National grid," *International Journal of Engineering Science Invention*, vol. 3, no. 4, pp. 55–59, 2014.

[20] I. A. Samuel, J. Katende, C. O. A. Awosope, and A. A. Awelewa, "Prediction of voltage collapse in electrical power system networks using a new voltage stability index," *International Journal of Applied Engineering Research*, vol. 2012, no. 2, pp. 190–199, 2017.

[21] M. Mathew, S. Ghosh, D. S. Babu, and A. A. Ansari, "An assessment of voltage stability based on line voltage stability indices and its enhancement using TCSC," *IOSR Journal of Electrical and Electronics Engineering (IOSR-JEEE)*, vol. 10, no. 6, pp. 81–88, 15AD.

[22] M. C. Pacis, I. J. M. Antonio, and I. J. T. Banaga, "Under voltage load shedding algorithm using fast voltage stability index (FVSI) and line stability index (LSI)," in *2021 IEEE 13th International Conference on Humanoid, Nanotechnology, Information Technology, Communication and Control, Environment, and Management (HNICEM)*, Nov. 2021, pp. 1–6, doi: 10.1109/HNICEM54116.2021.9731927.

[23] H. S. Mohsin Al-Wazni and S. S. Abdulla Al-Kubragyi, "A hybrid algorithm for voltage stability enhancement of distribution systems," *International Journal of Electrical and Computer Engineering (IJECE)*, vol. 12, no. 1, p. 50, Feb. 2022, doi: 10.11591/ijece.v12i1.pp50-61.

[24] H. Saeed Qazi, Z. Ullah, A. Alferidi, M. Alsolami, B. Lami, and S. M. Abrar Akber, "Stability analysis and voltage improvement in DG-integrated distribution networks using VCPI-based critical buses and lines detection considering uncertain power factor," *Ain Shams Engineering Journal*, vol. 15, no. 12, p. 103142, Dec. 2024, doi: 10.1016/j.asej.2024.103142.

[25] R. Kyomugisha, C. M. Muriithi, and G. N. Nyakoe, "Performance of various voltage stability indices in a stochastic multiobjective optimal power flow using Mayfly algorithm," *Journal of Electrical and Computer Engineering*, vol. 2022, pp. 1–22, Apr. 2022, doi: 10.1155/2022/7456333.

[26] I. Musirin and T. K. Abdul Rahman, "Novel fast voltage stability index (FVSI) for voltage stability analysis in power transmission system," in *Student Conference on Research and Development*, pp. 265–268, doi: 10.1109/SCORED.2002.1033108.

[27] A. Basit, "Temporary load shedding-optimization of power distribution system using load shedding techniques," Master Thesis, UiT The Arctic University of Norway, 2022.

[28] S. Mokred and Y. Wang, "Voltage stability assessment and contingency ranking in power systems based on modern stability assessment index," *Results in Engineering*, vol. 23, p. 102548, Sep. 2024, doi: 10.1016/j.rineng.2024.102548.
[29] I. M. Wartana, N. P. Agustini, and S. Sreedharan, "Improved security and stability of grid connected the wind energy conversion system by unified power flow controller," *Indonesian Journal of Electrical Engineering and Computer Science*, vol. 27, no. 3, p. 1151, Sep. 2022, doi: 10.11591/ijeecs.v27.i3.pp1151-1161.
[30] UP2B sistem Makassar, "Single line diagram sistem Subagsel," *Makassar: PLN Makassar*, 2024. https://drive.google.com/drive/folders/1h9VD-cjQqdfwUZcbEpN_BdcAQGYin5Sh (accessed Apr. 06, 2025).
[31] UP2B sistem Makassar, "Subbagsel system transmission channel data (in Bahasa)," *Makassar: PLN Makassar*, 2023. https://drive.google.com/file/d/1tnQgzAg-tdB6cNZK2lRlkxegrV_Iq2Sd/view?usp=drive_link (accessed Apr. 06, 2025).

BIOGRAPHIES OF AUTHORS

Andi Muhammad Ilyas received a Bachelor's degree in electrical engineering, Faculty of Engineering, Muslim University of Indonesia, Makassar, in 1995. In 2010, he received a Master of Engineering degree in electrical engineering, Postgraduate Program, Sepuluh Nopember Institute of Technology, Surabaya. In 2022, he received a Doctorate in the Department of Electrical Engineering, Faculty of Engineering, Hasanuddin University, Makassar. Currently, he is serving as a Lecturer in the Electrical Engineering Study Program, Faculty of Engineering, Khairun University. His research areas include optimal power flow, wind power generation, renewable energy, artificial intelligence applied power systems, power grids, power transmission reliability, wind power generation power forecasting. He can be contacted via email: aamilyas@gmail.com.

Agus Siswanto born in Demak Central Java, August 18, 1979, Indonesia. He learned a Bachelor of Engineering degree in electrical engineering from Darul Ulum University, Jombang, East Java, Indonesia in 2003. a Master of Engineering degree in electrical engineering from Sepuluh Nopember Institute of Technology, Surabaya, East Java, Indonesia in 2007. and a Doctor of Engineering degree in electrical engineering from Hasanuddin University, Makassar, Indonesia in 2020. He is interested in renewable energy, stability and control of electric power systems, wind turbines and smart grids. He can be contacted via email: asiswanto.untagcrb@gmail.com.

Muhammad Natsir Rahman received his B.Sc. from Hasanuddin University in electrical engineering, Faculty of Engineering, Makassar, in 1999. In 2004, he received a Master of Engineering in electrical engineering from the Institute of Technology Bandung, Bandung. Currently, he is serving as a Lecturer in the Electrical Engineering Study Program, Faculty of Engineering, Khairun University. His research areas include power quality, renewable energy, and artificial intelligence applied to electrical energy management. He can be contacted via email: mnr4hm4n@gmail.com.